J Incl Phenom Macrocycl Chem (2011) 71:331–337
DOI 10.1007/s10847-011-9967-9

ORIGINAL ARTICLE

Copper(II) and zinc(II) chemistry of a new hexadentate cyclam-based bis-di-2-pyridylmethanamine ligand

Peter Comba · Gerald Linti · Marta Zajaczkowski-Fischer · Thomas Zessin

Received: 1 April 2011 / Accepted: 4 April 2011 / Published online: 10 May 2011

Abstract In the *endo*-conformation of the substituted cyclam derivative L, with two *trans*-disposed di-2-pyridylmethanamine (dipa) coordination sites (*endo*: both dipa subunits on the same face of cyclam), the bis-dipa-substituted cyclam platform may form hexacoordinate mononuclear complexes with the two dipa subunits coordinated to one metal ion or dinuclear complexes, when the two dipa subunits are coordinated to two metal ions (oligonuclear linear chain complexes with *exo*-configured ligands L and metal ions coordinated to the cyclam unit have not been observed so far). Here, the structures, relative stabilities and spectroscopic properties of the mononuclear complexes of Cu^{II} and Zn^{II}, which are formed in preference to other structural possibilities, are discussed, and the preference for their formation is also evaluated.

Keywords Homoleptic complexes · N-substituted cyclam · Facially coordinated tridentate ligands · Di-2-pyridylmethanamine

Introduction

The substituted 1,7-dimethyl-1,4,7,11-tetraazacyclotetradecane (*trans*-dimethyl-cyclam) macrocycle L with two bis-di-2-pyridylmethanamine (dipa) side chains (L in Scheme 1), was designed by qualitative molecular modeling, as a dinucleating ligand for purple acid phosphatase (PAP) model complexes, where the secondary interactions (hydrogen bond donors positioned at the cyclam platform) help to position the phosphomonoester substrate for an efficient ester hydrolysis [1]. This design was based on a structural model of the active site (see Scheme 2a), derived from mechanistic studies, involving enzyme kinetics, enzyme structural work and quantum chemical studies (DFT and QM-MM) [2–5]. Indeed, the oxo-bridged diferric complex of L is the first PAP model, which is able to mimic the biological activity, i.e., it hydrolyzes phosphomonoesters (see Scheme 2b), in contrast to other PAP model systems, which only hydrolyze phosphodiesters. [1]

The synthesis of L (see Scheme 1) involves the well known *trans*-difunctionalization of cyclam [6], to yield the *trans*-2-aminoethyl-substituted dimethyl-cyclam platform, which is alkylated with dipyridylmethylchloride [7] to pale yellow crystals of L (14% overall yield in the six-step synthesis from cyclam and dipyridylmethylchloride).

Not unexpectedly, due to the flexibility of the two tridentate coordination sites, and without a ligand-based bridging group between the two metal centers, which usually is present in this type of model systems [2, 8, 9] but not in the metalloprotein, the synthesis of dinuclear systems turned out to be difficult. In fact, the only dinuclear complex isolated so far is the diferric system, where the success of the synthetic procedure is based on an oxo-bridged diferric iron source, derived from $[FeCl_4](NEt_4)$ in wet basic MeCN solution [1, 10]. All other attempts to prepare dinuclear complexes lead to the formation of

We dedicate this publication to Prof. Leonard F. Lindoy in celebration of his 75th birthday.

Electronic supplementary material The online version of this article (doi:10.1007/s10847-011-9967-9) contains supplementary material, which is available to authorized users.

P. Comba (✉) · G. Linti · M. Zajaczkowski-Fischer · T. Zessin
Anorganisch-Chemisches Institut, INF 270, Universität Heidelberg, 69120 Heidelberg, Germany
e-mail: peter.comba@aci.uni-heidelberg.de

Scheme 1 Synthesis of the ligand L [1]

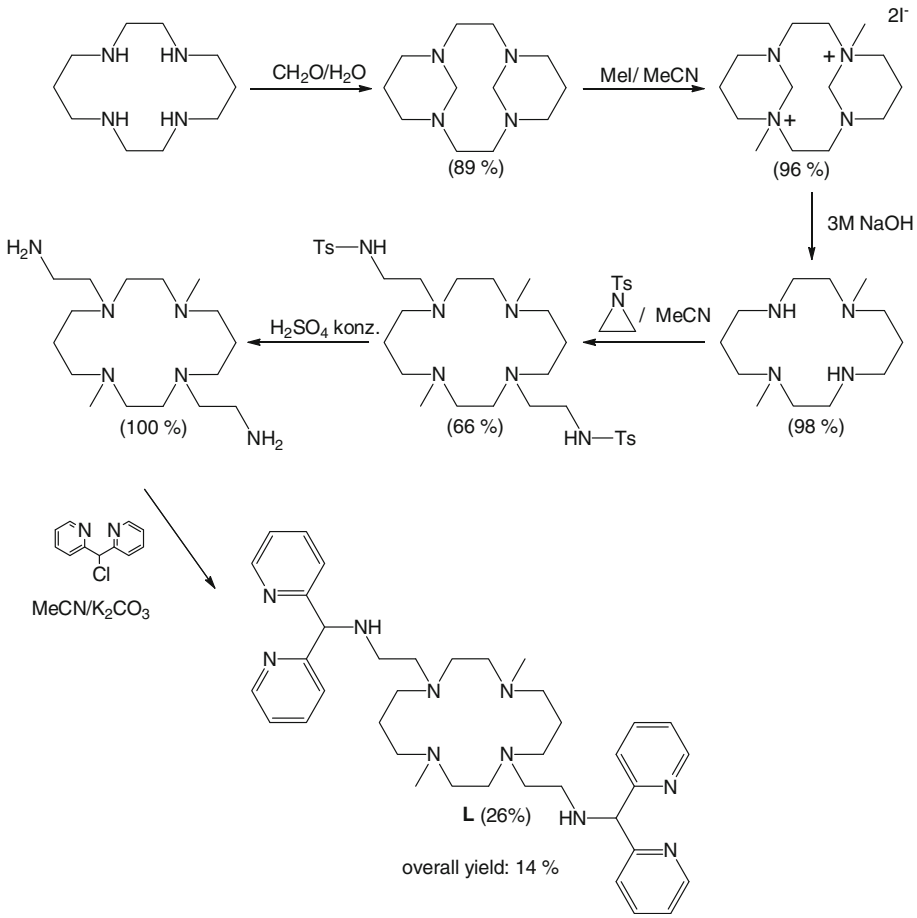

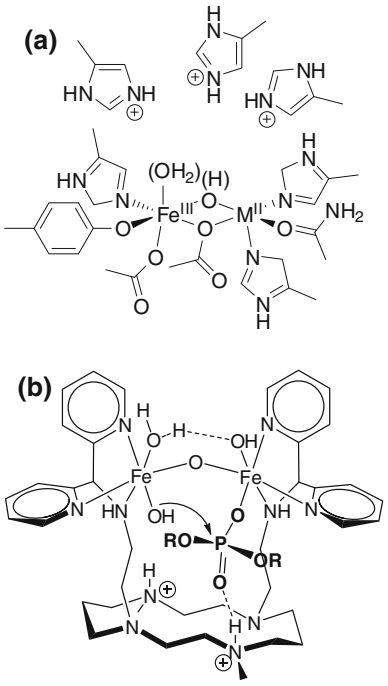

Scheme 2 **a** The PAP active site and **b** the L-based PAP model [1]

hexacoordinate mononuclear $[M(L)]^{n+}$ complexes with the two amine-dipyridyl subunits of L coordinated to a single metal ion. Interestingly, no complexes with metal ions coordinated to the macrocyclic cavity (tetraalkyl-cyclam) were isolated so far. The Cu^{II} and Zn^{II} complexes of L are discussed in this communication.

Results and discussion

Reaction of stoichiometric amounts of L and $Cu(Otf)_2$ or $Zn(Otf)_2$ (Otf = trifluoromethanesulfonate, $CF_3SO_3^-$) in dry MeCN (room temperature, inert conditions, reaction time less than 1 h) and subsequent diffusion of diethylether into the solution lead to crystals of the two complexes, which were suitable for X-ray crystallography and were also used for the analyses and spectroscopic characterization. These compounds are derived from the known complexes of the facially coordinating tridentate ligand dipyridylmethylamine (dipa), which forms conformationally rigid, homoleptic octahedral complexes. These occur in two isomers, the *rac*-form with *cis*-disposed secondary

amine groups, and the *meso*-form with an all-*trans*-configuration [11]; in general, due to steric interactions, the former is more stable. Interestingly, the crystal structure analysis of $[Cu(dipa)_2]^{2+}$ shows the molecular cation to be in the less stable *meso*-configuration, and with one of the two py–Cu–py axes elongated (2.536 vs. 2.021 Å), while the secondary amines have distances (2.020 Å) as expected for in-plane Cu^{II}–NH_2 bonds. From the isolated and therefore *meso*-configurated $[Cu(dipa)_2]^{2+}$ complex, a hexadentate ligand coordinated to Cu^{II} ($[Cu(mnpdipa)]^{2+}$, mnpdipa = 4-methyl-4-nitro-1,1′,7,7′-tetra-2pyridyl-2,6-diazaheptane) is obtained in a one-pot Sargeson-type template condensation—a reaction which was extensively used in Cu^{II}-mediated syntheses of open-chained and macrocyclic ligands [12, 13]. The two hexadentate ligands mnpdipa and L have similar structures, i.e., the two dipa subunits in *meso*-$[Cu(dipa)_2]^{2+}$ are coordinated to Cu^{II} with *trans*-disposed amine donors and to some degree, the complex isomerizes prior to the template condensation to form $[Cu(mnpdipa)]^{2+}$ [11].

The metal-free ligand L may occur in two diametrically different forms, i.e., with the two appended donor groups on the same or on different sides of the cyclam platform (*endo* or *exo*, respectively; note that for each of these geometries, there are many different conformations). For both coordination modes known so far (the diferric PAP model complex [1] and the Cu^{II} and Zn^{II} complexes discussed here), the ligand needs to be in the *endo* form. The conformational space was searched by force-field based methods (for details, see "Experimental" section), and the two most stable structures are shown in Fig. 1a and b. These are nearly degenerate (with a 2 kJ/mol preference for the *endo* form), and all other found conformers adopt energies within only 8 kJ/mol. This is as expected for the highly flexible ligand L.

The metal-free ligand L and its diprotonated form $[H_2L]^{2+}$ were crystallized and both structures were solved (Table 1; Fig. 1c and d). There is a preference for *exo* structures in the crystal lattice, yielding C_i symmetry (triclinic space group) in the non-protonated, and C_{2h} symmetry (monoclinic space group) in the protonated ligand. An *endo* structure would lead to lower symmetry and less favorable crystal packing. There are small structural differences between L and its protonated form: in the latter, the dipa binding pockets are rotated such that the two pyridine groups face the doubly-protonated cyclam ring, which is in an all-pseudo-chair conformation in both structures.

The experimental structures of $[Zn(L)](Otf)_2$ and $[Cu(L)](Otf)_2$ were also analyzed by X-ray diffraction. Plots of the molecular cations are presented in Fig. 2 and the important geometric parameters are listed in Table 1. The two structures confirm the coordination mode of the hexadentate ligand and the geometric data, especially the metal-donor distances are in the expected ranges [14]. The Cu^{II} and Zn^{II} structures are very similar to each other with the expected difference that the Cu^{II} complex has one axis with a strong Jahn-Teller elongation. Interestingly, this is along one of the two N_{amine}–Cu–$N_{pyridine}$ axes, with the

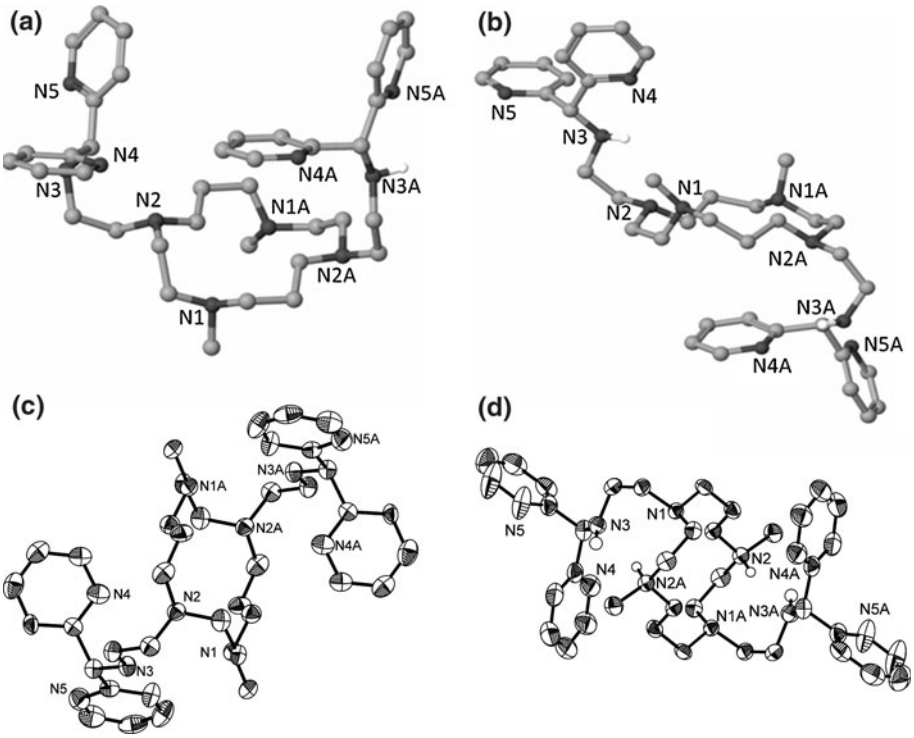

Fig. 1 Lowest-energy conformers from conformational search on L (**a** and **b**) and Ortep plots of the X-ray structures of **c** L and **d** $[H_2L]^{2+}$ (ellipsoids are drawn at 50% prob. level)

Table 1 Selected structural parameters (distances in Å, angles in °) of $[Cu(L)](Otf)_2$ and $[Zn(L)](Otf)_2$

Parameter	$[Cu(L)](Otf)_2$	$[Zn(L)](Otf)_2$
M–N5	2.528(3)	2.185(3)
M–N8	2.074(3)	2.233(3)
M–N6	2.029(3)	2.190(3)
M–N7	2.016(3)	2.148(3)
M–N9	2.405(3)	2.146(3)
M–N10	2.002(3)	2.164(3)
N5–M–N8	112.77(12)	115.08(13)
N5–M–N6	73.26(11)	75.87(12)
N5–M–N7	75.73(10)	77.05(12)
N5–M–N9	170.72(10)	168.66(11)
N8–M–N6	172.14(12)	165.48(12)
N7–M–N10	176.61(11)	177.16(11)

corresponding $Cu–N_{amine}$ bond at 2.50 vs. 2.07 Å, and the $Cu–N_{pyridine}$ bond at 2.40 vs. 2.00 Å. Based on the *meso*-$[Cu(dipa)]^{2+}$ structure [11], the expectation is that the "Jahn-Teller isomer" [15, 16] with an elongation along $N_{pyridine}–Cu–N_{pyridine}$ is close to degenerate with rather low activation barriers between the various minima [17].

An interesting question is, why L strictly prefers the coordination mode described in this communication, i.e. why (i) coordination to the cyclam subunit and (ii) the formation of dinuclear complexes is disfavored. Notably, cyclam leads to very stable Cu^{II} (and Zn^{II}) complexes. However, these are in the generally preferred *trans*-III configuration (similar to the conformation observed in the metal-free ligands, see Fig. 1b) [18]. With the four-fold N-substituted cyclam derivatives (e.g., *N*,*N*′,*N*″,*N*‴-tetramethyl-cyclam (tmc) and the ligand L discussed here), the *trans*-I configuration is preferred [19–21], and this is known to lead to considerably smaller complex stabilities (for Ni^{II} the complex stabilities (log *K* values) with cyclam and tmc are 20.1 and 8.6; note that the log *K* values of Cu^{II} with cyclam and dipa are 26 and 16.8 [log β (brutto stability constant, log $K_1 = 8.9$; log $K_2 = 7.9$)], that with tmc is around 18 [11, 22–24]. Therefore, based on these relative and rather crude values for complex stabilities, there is at most a small thermodynamic preference for the coordination of metal ions to the macrocyclic site. More importantly, the kinetically preferred site is the well preorganized bis-dipa subunit since complexation of macrocyclic cavities, in particular of cyclam derivatives in the *trans*-I conformation, is not a facile process (the difference in rate of formation is assumed to be around 30,000-fold) [25].

The similarity between L and mnpdipa extends to the ligand field and EPR spectra with parameters listed in Table 2. These data suggest that hexacoordination is retained in solution. As suggested before, due to similar bonding properties of amine and pyridine donors, the two possible orientations of the dipa units in $[Cu(dipa)]^{2+}$ (*rac* and *meso*) are not expected to lead to significant differences in the ligand field and EPR spectra [11]. The higher flexibility of the cyclam-based ligand L, as compared to the rather tight propylene-bridged hexadentate mnpdipa and the bis-tridentate complex with dipa leads to a significantly lower ligand field, and this is the result of the structural differences discussed above, i.e., a lower symmetry and slightly longer in-plane $Cu^{II}–N$ bond distances.

Experimental

Chemicals

Solvents for organic synthesis were of standard quality and distilled prior to use. Solvents for complex synthesis and spectroscopy were of p.a. grade and used without further purification. Dry solvents were purchased form Sigma-Aldrich, stored over molecular sieves and used without further purification. Cyclam was purchased from ChemaTech, other chemicals from Sigma-Aldrich. 1,8-Dimethylcyclam

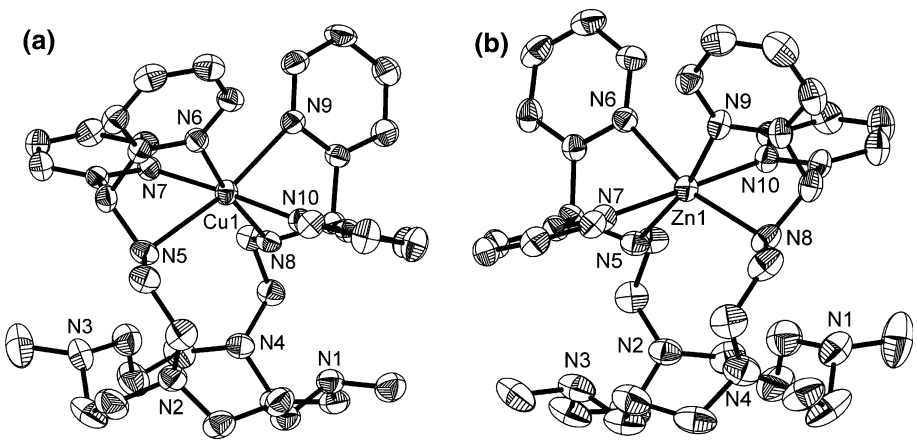

Fig. 2 Ortep plots of the X-ray structures of **a** $[Cu(L)](Otf)_2$ and **b** $[Zn(L)](Otf)_2$ (hydrogen atoms are omitted for clarity; ellipsoids are drawn at 50% probability level)

Table 2 Comparison of spectroscopic parameters of $[Cu(L)]^{2+}$, $[Cu(dipa)_2]^{2+}$ (*trans*-configuration) and $[Cu(mnpdipa)]^{2+}$ (*cis*-configuration of the amine donors, similar to the geometry observed in $[Cu(L)]^{2+}$) [11]

	λ_{max} (dd) (nm)	$g_{\|}$	$g\perp$	$A_{\|}$ ($\times 10^{-4}$ cm^{-1})	$A\perp$ ($\times 10^{-4}$ cm^{-1})
$[Cu(L)]^{2+}$	639	2.23	2.05	180	n.a.
$[Cu(dipa)_2]^{2+}$	616	2.23	2.08	188	23
$[Cu(mnpdipa)]^{2+}$	605	2.22	2.09	187	21

[6], *N*-tosylaziridine [26, 27] and di-(2-pyridyl)methyl chloride [7] were synthesized according to literature procedures.

Characterization

UV/Vis spectra were recorded on a JASCO V-570 spectrophotometer equipped with a JASCO ETC.-505T cryostat at 25 °C. NMR spectra were recorded at 399.89 MHz (^{1}H), and 100.55 MHz (^{13}C) on a Bruker Avance II 400 instrument. For ^{1}H and ^{13}C spectra, the respective solvent peak was used as reference for the chemical shift δ. All reported coupling constants ^nJ are for ^{1}H–^{1}H couplings. The following abbreviations are used for signal multiplicities: s = singlet, bs = broad singlet, d = doublet, t = triplet, q = quartet, quin = quintet, dd = doublet of doublets, ddd = doublet of doublets of doublets, dt = doublet of triplets, tt = triplet of triplets, m = multiplet. IR spectra were obtained with a Perkin Elmer 16 PC FT-IR spectrometer in KBr. Signal intensities are abbreviated as followed: b = broad, w = weak, m = medium, s = strong. X-band EPR spectra (ca. 9 GHz) at liquid nitrogen temperature were recorded on a Bruker Biospin ELEXSYS E500 spectrometer with a Super High Q cavity located at the Institute of Inorganic Chemistry (University Heidelberg). In the case of liquid nitrogen cooling, an ITC4 temperature controller was used. Spin-Hamiltonian parameters were determined from computer simulation of the experimental spectra using MoSophe [28]. The simulated and experimental spectra were visualized with Xepr [29]. FAB mass spectra were measured on a Finnigan TSQ 700 instrument with nitrobenzylalcohol as matrix at the Institute of Inorganic Chemistry at the University of Heidelberg. HR-ESI mass spectra were measured on a Bruker Apex-Qe hybrid 9.4 T FT-ICR instrument at the Institute of Organic Chemistry at the University of Heidelberg. Elemental analyses were performed in the analytical laboratories of the Chemical Institutes at the University of Heidelberg on an Elementar Vario EL instrument.

Syntheses

Ligand L. This ligand was prepared in six steps from cyclam in 14% overall yield according to a published method [1]. ^{1}H-NMR (400 MHz, $CDCl_3$): δ = 8.53 (dd, $^3J_{H,H}$ = 4.8 Hz, $^4J_{H,H}$ = 1.2 Hz, 4H, C*H*$_{ar}$N), 7.60 (dt, $^3J_{H,H}$ = 8.0 Hz, $^4J_{H,H}$ = 1.2 Hz, 4H, C*H*$_{ar}$ para to N), 7.48 (d, 4H, C*H*$_{ar}$C$_q$), 7.10 (ddd, 4H, $^3J_{H,H}$ = 8.0 Hz, $^3J_{H,H}$ = 4.8 Hz, $^4J_{H,H}$ = 1.2 Hz, C*H*$_{ar}$CHN), 5.06 (s, 2H, C*H*py$_2$), 3.12 (bs, 2H, N*H*), 2.7–2.2 (m, 24H, all N–C*H*$_2$), 2.11 (s, 6H, N–C*H*$_3$), 1.47 (quin, 4H, $^3J_{H,H}$ = 6.8 Hz, 4H, C–C*H*$_2$–C). ^{13}C-NMR (100 MHz, $CDCl_3$): δ = 161.9 (*C*$_{ar,q}$), 149.2, 136.5, 122.2, 122.0 (*C*$_{ar}$), 70.3 (*C*Hpy$_2$), 54.5, 54.3, 53.9, 51.7, 50.8 (all N–*C*H$_2$), 45.7 (*C*H$_2$–NH), 43.5 (N–*C*H$_3$), 24.1 (C–*C*H$_2$–C). IR (KBr): $\tilde{\nu}$ [cm^{-1}] = 3439 (b), 3282 (m), 2981 (m), 2937 (m), 2846 (m), 2792 (s), 1674 (s), 1565 (s), 1599 (m), 1473 (s), 1466 (s), 1435 (s), 1294 (m), 1162 (m), 1125 (m), 1114 (m), 999 (w), 929 (m), 887 (w), 809 (m), 771 (m). FAB$^+$-MS (nibeol): *m/z* (%): 651.6 (97) $[M+H]^+$. Elemental analysis (%): calc. for $C_{38}H_{54}N_{10}\cdot H_2O$: C, 68.23; H, 8.44; N, 20.94; found: C, 68.69; H, 8.43; N, 21.05.

[Zn(L)](Otf)$_2$. Ligand L (32.5 mg, 0.05 mmol) and $Zn(Otf)_2$ (18.2 mg, 0.05 mmol) are stirred in dry MeCN (9 mL) for 1 h at ambient temperature. Diffusion of diethylether into the solution yields colorless crystals of the Zn^{II} complex (0.05 g, 96%), suitable for X-ray crystallography. HR-ESI$^+$-MS (MeCN): *m/z* (%): 357.19138 (calc. 357.19122) (87) $[Zn(L)]^{2+}$; 863.33451 (863.33446) (61) $[Zn(L)(Otf)]^+$. Elemental analysis (%): calc. for $C_{40}H_{54}N_{10}O_6S_2F_6Zn\cdot 1/3\ Zn(OH)_2$: C, 45.86; H, 5.26; N, 13.37; found: C, 45.90; H, 5.13; N, 13.00.

[Cu(L)](Otf)$_2$. Ligand L (32.5 mg, 0.05 mmol) and $Cu(Otf)_2$ (18.1 mg, 0.05 mmol) are stirred in dry MeCN (4 mL) for 1 h at ambient temperature. Diffusion of diethylether into the solution yields blue crystals of the Cu^{II} complex (50.0 mg, 95%), suitable for X-ray crystallography. HR-ESI$^+$-MS (MeCN): *m/z* (%): 356.69148 (calc. 356.69145) (100) $[Cu(L)]^{2+}$; 431.67117 (calc. 431.67137) (98) $[Cu(HL)(Otf)]^{2+}$; 862.33687 (calc. 862.33492) (20) $[Cu(L)(Otf)]^+$. UV/Vis (MeCN): λ_{max} [nm] (ε [M^{-1} cm^{-1}]) = 639 (45). EPR (MeCN/buffer pH 6 1:1): $g_{\|}$ = 2.23; $g\perp$ = 2.05; $A_{\|}$ = 180 × 10^{-4} cm^{-1}. Elemental analysis (%): calc. for: $C_{42}H_{57}N_{11}O_6S_2F_6Cu$: C, 47.88; H, 5.45; N, 14.62; found: C, 47.29; H, 5.47; N, 14.30.

Crystallography

X-ray data for single-crystals were collected on an STOE IPDS I diffractometer equipped with an image plate area detector, using a graphite monochromator Mo(Kα)

Table 3 Crystal data and structure refinement details

Compound	L	$[H_2L]^{2+}$	$[Cu(L)](Otf)_2$	$[Zn(L)](Otf)_2$
Chemical formula	$C_{38}H_{58}N_{10}O$	$C_{42}H_{62}Cl_2N_{12}O_8$	$C_{42}H_{57}CuF_6N_{11}O_6S_2$	$C_{40}H_{54}F_6N_{10}O_6S_2Zn$
M (g mol^{-1})	686.94	933.94	1053.65	1014.42
Crystal system	Triclinic	Monoclinic	Monoclinic	Monoclinic
Space group	$P\bar{1}$	$P2_1/c$	$P2_1/c$	$P2_1/c$
a (Å)	8.4924(17)	14.210(3)	11.157(2)	13.873(3)
b (Å)	10.681(2)	8.8923(18)	30.396(6)	17.163(3)
c (Å)	11.126(2)	18.919(4)	14.021(3)	19.895(4)
α (°)	102.85(3)			
β (°)	93.32(3)	101.59(3)	92.15(3)	104.08(3)
γ (°)	108.57(3)			
V (Å^3)	923.6(3)	2341.9(8)	4751.4(16)	4594.8(16)
Z	1	2	4	4
Dc (g cm^{-3})	1.235	1.324	1.473	1.466
μ(MoKα) (mm^{-1})	0.079	0.203	0.630	
Absorption corr.	Numerical	Numerical	Numerical	Numerical
$T_{min,max}$	0.9812/0.9918	0.9009/0.9659	0.8033/0.8981	0.7596/0.8577
F(000)	372	992	2196	2112
Crystal size (mm^3)	0.235 × 0.228 × 0.100	0.37 × 0.26 × 0.14	0.50 × 0.35 × 0.22	0.67 × 0.28 × 0.26
Θ (°)	1.90–22.47	2.20–26.12	1.95–26.15	2.28–28.22
hkl range	$-9 \le h \le 9$	$-17 \le h \le 17$	$-13 \le h \le 13$	$-18 \le h \le 18$
	$-11 \le k \le 11$	$-10 \le k \le 10$	$-37 \le k \le 37$	$-22 \le k \le 22$
	$-11 \le l \le 11$	$-23 \le l \le 22$	$-17 \le l \le 17$	$-26 \le l \le 24$
N	4951	18,200	37,943	44,907
N_{ind}	2274	4614	9345	10,518
N_{obs} ($I > 2\sigma(I)$)	1033	2324	4651	5522
N_{restr}/N_{par}	2/238	21/334	0/622	0/604
GoF(all)	0.830	0.797	0.769	0.750
$R_1(F)$ ($I > 2\sigma(I)$)	0.066	0.0477	0.0470	0.0610
$wR_2(F^2)$ ($I > 2\sigma(I)$)	0.1503	0.1077	0.0885	0.1609
$R_1(F)$ (all data)	0.1324	0.0974	0.1015	0.1099
$wR_2(F^2)$ (all data)	0.1705	0.1192	0.0979	0.1869
$\Delta\rho_{max}$ (eÅ^{-3})	0.340	0.439	0.526	2.586
$\Delta\rho_{min}$ (eÅ^{-3})	−0.269	−0.437	−0.303	−0.616

($\lambda = 0.71073$ Å). The structure was refined against all F^2 data by full-matrix least squares techniques (SHELXTL 5.01; PC Version, Bruker AXS) [30]. All non-hydrogen atoms were refined with anisotropic thermal parameters. All H atoms were placed in calculated positions and refined using a riding model. Crystal data and structure refinement details are given in Table 3. The molecular plots were produced with Diamond. CCDC 819253–819256 include the supplementary crystallographic data. These can be obtained free of charge via www.ccdc.cam.ac.uk.

Conformational search

Conformational searches of L were done with Macromodel 9.6, using Maestro 8.5.111 [31]. The torsional sampling procedure (Monte Carlo multiple minima) with 1000 steps was used to produce between 50 and 200 different structures, which were subsequently geometry-optimized in up to 50,000 iterations (MM3* force field [32], steepest descent, gradient convergence threshold = 0.01).

Acknowledgment Financial support by the German Science Foundation (DFG) and the University of Heidelberg is gratefully acknowledged.

References

1. Comba, P., Gahan, L.R., Mereacre, V., Hanson, G.R., Powell, A.K., Schenk, G., Zajaczkowski-Fischer, M.: Monoesterase

activity of a purple acid phosphatase mimic with a cyclam platform. Chem. Eur. J. (2011) (submitted)
2. Mitic, N., Smith, S.J., Neves, A., Guddat, L.W., Gahan, L.R., Schenk, G.: The catalytic mechanisms of binuclear metallohydrolases. Chem. Rev. **106**, 3338–3363 (2006)
3. Schenk, G., Elliott, T.W., Leung, E., Carrington, L.E., Mitic, N., Gahan, L.R., Guddat, L.W.: Crystal structures of a purple acid phosphatase, representing different steps of this enzyme's catalytic cycle. BMC Struct. Biol. **8**, 6 (2008)
4. Alberto, M.E., Marino, T., Ramos, M.J., Russo, N.: Atomistic details of the catalytic mechanism of Fe(III)-Zn(II) purple acid phosphatase. J. Chem. Theory Comput. **6**, 2424–2433 (2010)
5. Bosch, S., Comba, P., Zajazckowski-Fischer, M. (in preparation)
6. Royal, G., Dahaoui-Gindrey, V., Dahaoui, S., Tabard, A., Guilard, R., Pullumbi, P., Lecomte, C.: New synthesis of *trans*-disubstituted cyclam macrocycles—elucidation of the disubstitution mechanism on the basis of X-ray data and molecular modeling. Eur. J. Org. Chem. **9**, 1971–1975 (1998)
7. Roelfes, G., Vrajmasu, V., Chen, K., Ho, R.Y.N., Rohde, J., Zondervan, C., la Crois, R.M., Schudde, E.P., Lutz, M., Spek, A.L., Hage, R., Feringa, B., Munck, E., Que Jr., L.: End-on and side-on peroxo derivatives of non-heme iron complexes with pentadentate ligands: models for putative intermediates in biological iron/dioxygen chemistry. Inorg. Chem. **42**, 2639–2653 (2003)
8. Than, R., Feldmann, A.A., Krebs, B.: Structural and functional studies on model compounds of purple acid phosphatases and catechol oxidases. Coord. Chem. Rev. **182**, 211–241 (1999)
9. Gahan, L.R., Smith, S.J., Neves, A., Schenk, G.: Phosphate ester hydrolysis: metal complexes as purple acid phosphatase and phosphotriesterase analogues. Eur. J. Inorg. Chem. **19**, 2745–2758 (2009)
10. Armstrong, W.H., Lippard, S.J.: Convenient, high-yield synthesis of tetraethylammonium (μ-oxo)bis[trichloroferrate(III)] $(Et_4N)_2[Fe_2OC_{l6}]$). Inorg. Chem. **24**, 981 (1985)
11. Bernhardt, P.V., Comba, P., Mahu-Rickenbach, A., Stebler, S., Steiner, S., Várnagy, K., Zehnder, M.: Transition metal complexes of the novel tridentate di-2-pyridylmethanamine (dipa). Inorg. Chem. **31**, 4194 (1992)
12. Comba, P., Hambley, T.W., Lawrance, G.A., Martin, L.L., Renold, P., Várnagy, K.: Template syntheses of chiral tetradentate ligands derived from L-amino acids. Characterization of their copper(II) complexes. J. Chem. Soc. Dalton Trans. 277 (1991)
13. Comba, P., Curtis, N.F., Lawrance, G.A., Sargeson, A.M., Skelton, B.W., White, A.H.: Template synthesis involving carbon acids. Synthesis and characterization of (3,10-dimethyl-3,10-dinitro-1,4,8,11-tetraazacyclotetradecane)copper(II) and (1,9-diamino-5-methyl-5-nitro-3,7-diazanonane)copper(II) cations and nitro group reduction products. Inorg. Chem. **25**, 4260 (1986)
14. Orpen, A.G., Brammer, L., Allen, F.H., Kennard, O., Watson, D.G., Taylor, R.: Tables of bond lengths determined by X-ray and neutron-diffraction. 2. Organometallic compounds and co-ordination complexes of the d-block and f-block metals. J. Chem. Soc. Dalton Trans. S1–S83 (1989)
15. Comba, P., Hauser, A., Kerscher, M., Pritzkow, H.: Bond-stretch isomerism: trapped isomeric structures of hexacoordinate copper(II) bispidine chromophores along a Jahn-Teller active vibrational coordinate. Angew. Chem. Int. Ed. **42**, 4536–4540 (2003)
16. Born, K., Comba, P., Kerscher, M., Rohwer, H.: Distortional isomerism with copper(I) complexes of tetradentate 3,7-diazabicyclo[3.3.1]nonane derivatives. Dalton Trans. 362 (2009)
17. Comba, P., Pandian, S., Wadepohl, H., Wiesner, S.: Structures, spectroscopy and modeling of a rare set of isomeric copper(II) complexes. Inorg. Chim. Acta (2011) (in press)
18. Bosnich, B., Poon, C.K., Tobe, M.L.: Complexes of cobalt(III) with a cyclic tetradentate secondary amine. Inorg. Chem. **4**, 1102–1108 (1965)
19. Barefield, E.K., Wagner, F.: Metal complexes of 1,4,8,11-tetraazacyclotetradecane, N-tetramethylcyclam. Inorg. Chem. **12**, 2435 (1973)
20. Hambley, T.W.: The crystal structure of R,S,R,S-(1,4,8,11-tetramethyl-1,4,8,11-tetraazacyclotetradecane)nickel(II) bis(trifluoromethanesulphonate)-acetone hydrate, $[Ni(tmtactd)][CF_3SO_3]_2 \cdot Me_2CO \cdot H_2O$, and a strain-energy minimization analysis of four-, five-, and six-co-ordinate nickel(II)-tmtactd solvento complexes. J. Chem. Soc. Dalton Trans. 565–569 (1986)
21. Comba, P., Jurisic, P., Lampeka, Y.D., Peters, A., Prikhod'ko, A.I., Pritzkow, H.: Axial bonds in copper(II) compounds. Inorg. Chim. Acta **324**, 99 (2001)
22. Hancock, R.D., Martell, A.E.: The chelate, cryptate and macroyclic effects. Comments Inorg. Chem. **6**, 237 (1988)
23. Nakani, B.S., Hancock, R.D.: The chelate, cryptate and macroyclic effects. S. Afr. J. Chem **36**, 117 (1983)
24. Hertli, L., Kaden, T.A.: Metal complexes with macrocyclic ligands, V. Formation and dissociation kinetics of the pentacoordinated Ni^{2+}, Cu^{2+}, Co^{2+} and Zn^{2+} complexes with 1,4,8,11-tetramethyl-1,4,8,11-tetraazacyclotetradecane. Helv. Chim. Acta **57**, 1328–1333 (1974)
25. Kaden, T.: Komplexe mit makrocyclischen Liganden I. Mechanismus der Komplexbildung zwischen Ni^{2+} und 1,4,8,11-Tetraazacyclotetradecan. Helv. Chim. Acta **53**, 617 (1970)
26. Hope, D.B., Horncastle, K.C.: Synthesis of some dibasic sulphur-containing amino-acids related to L-lysine. J. Chem. Soc. C 1098–1101 (1966)
27. Martin, A.E., Ford, T.M., Bulkowski, J.E.: Synthesis of selectively protected tri- and hexaamine macrocycles. J. Org. Chem. **47**, 412–415 (1982)
28. Hanson, G.R., Noble, C.J., Benson, S.: Molecular sophe: an integrated approach to the structural characterization of metalloproteins: the next generation of computer simulation software. In: Hanson, G.R., Berliner, L.J. (eds.) High Resolution EPR: Applications to Metalloenzymes and Metals in Medicine, vol. 28, pp. 105–174. Springer, New York (2009)
29. Hanson, G.R., Gates, K.E., Noble, C.J., Griffin, M., Mitchell, A., Benson, S.: XSophe-Sophe-XeprView. A computer simulation software suite (v. 1.1.3) for the analysis of continuous wave EPR spectra. J. Inorg. Biochem. **98**, 903–916 (2004)
30. Sheldrick, G.M.: SHELXTL User's Manual. Siemens Analytical X-Ray Instruments Inc., Madison (1994)
31. Macromodel. Schrödinger, New York (2005)
32. Allinger, N.L., Yuh, Y.H., Lii, J.-H.: Molecular mechanics. The MM3 force field for hydrocarbons. 1. J. Am. Chem. Soc. **111**, 8551 (1989)